12-2021

# Evolving Tropical Cyclone Tracks in the North Atlantic in a Warming Climate

Andra J. Garner
*Rowan University*, garnera@rowan.edu

Robert Kopp

Benjamin Horton



## Recommended Citation

Garner, A. J., Kopp, R. E., & Horton, B. P. (2021). Evolving tropical cyclone tracks in the North Atlantic in a warming climate. Earth's Future, 9(12).

Earth's Future

RESEARCH ARTICLE
10.1029/2021EF002326

**Key Points:**

- Tropical cyclone (TC) characteristics (genesis, tracks, and termination) vary from pre-industrial to modern to future high-emissions climates
- More TCs travel within 100 km of Boston and Norfolk than New York City under a high-emissions future
- From the pre-industrial era to 2100 CE (high emissions), US east coast cities see reduced TC warning times and longer duration

**Supporting Information:**

Supporting Information may be found in the online version of this article.

**Correspondence to:**

A. J. Garner,
garnera@rowan.edu

**Citation:**

Garner, A. J., Kopp, R. E., & Horton, B. P. (2021). Evolving tropical cyclone tracks in the North Atlantic in a warming climate. *Earth's Future*, *9*, e2021EF002326. https://doi.org/10.1029/2021EF002326

Received 3 MAY 2021
Accepted 8 OCT 2021

**Author Contributions:**

**Conceptualization:** Andra J. Garner, Robert E. Kopp, Benjamin P. Horton
**Formal analysis:** Andra J. Garner
**Funding acquisition:** Andra J. Garner, Robert E. Kopp, Benjamin P. Horton
**Investigation:** Andra J. Garner
**Methodology:** Andra J. Garner
**Resources:** Andra J. Garner
**Visualization:** Andra J. Garner
**Writing – original draft:** Andra J. Garner, Robert E. Kopp, Benjamin P. Horton
**Writing – review & editing:** Andra J. Garner, Robert E. Kopp, Benjamin P. Horton



# Evolving Tropical Cyclone Tracks in the North Atlantic in a Warming Climate

**Andra J. Garner[1], Robert E. Kopp[2,3], and Benjamin P. Horton[4,5]**

[1]Department of Environmental Science, Rowan University, Glassboro, NJ, USA, [2]Department of Earth and Planetary Sciences, Rutgers University, Piscataway, NJ, USA, [3]Rutgers University, Institute of Earth, Ocean, and Atmospheric Sciences, New Brunswick, NJ, USA, [4]Asian School of the Environment, Nanyang Technological University, Singapore, [5]Earth Observatory of Singapore, Nanyang Technological University, Singapore

**Abstract** Tropical cyclone (TC) track characteristics in a changing climate remain uncertain. Here, we investigate the genesis, tracks, and termination of >35,000 synthetic TCs traveling within 250 km of New York City (NYC) from the pre-industrial era (850–1800 CE) to the modern era (1970–2005 CE) to the future (2080–2100 CE). Under a very high-emissions scenario (RCP8.5), TCs are more likely to form closer to the United States (U.S.) southeast coast (>15% increase), terminate in the northeastern Atlantic (>6% increase), and move most slowly along the U.S. Atlantic coast (>15% increase) from the pre-industrial to future. Under our modeled scenarios, TCs are more likely to travel within 100 km of Boston, MA, USA ($p = 0.01$) and Norfolk, VA, USA ($p = 0.05$) than within 100 km of NYC in the future. We identify reductions in the time between genesis and the time when TCs come within 100 km of NYC, Boston, or Norfolk, as well as increased duration of TC impacts from individual storms at all three cities in the future.

**Plain Language Summary** Future economic and human costs of tropical cyclones (TCs; i.e., hurricanes) will depend upon changing storm tracks. To better understand the potential hazard facing coastal communities along the United States (U.S.) Atlantic coast, >35,000 TCs are simulated under pre-industrial, modern, and very high-emissions future climates. Over time, TCs tend to travel closer to the cities of Boston and Norfolk than New York City (NYC). As the climate warms, TCs also form closer to the United States southeast coast, reach their slowest forward speed along the U.S. Atlantic coast, and persist farther north and east in the Atlantic basin. The time required for TCs to reach cities, such as Boston, Norfolk, and NYC is reduced, and the typical duration of TC conditions increases at each of these locations.

## 1. Introduction

Tropical cyclones (TCs) are the most damaging natural hazards to impact the Atlantic and Gulf coasts of the United States (U.S.; Emanuel, 2005; Pielke, 2007; Rappaport, 2014). From 2010 to 2020, U.S. coastlines were impacted by 19 TCs that qualified as billion-dollar disasters, causing a cumulative estimated cost of more than $480 billion (2020 inflation-adjusted), and more than 3,500 deaths (NOAA National Centers for Environmental Information (NCEI), 2020). These storms included damaging events, such as Hurricane Sandy (2012), Hurricanes Harvey, Irma, and Maria (2017), and Hurricane Dorian (2019).

In a warming climate, future economic and human costs of TCs in the U.S. will be determined not only by social and economic behaviors, but also by evolving TC characteristics (Emanuel, 2011; Grinsted et al., 2019; Mendelsohn et al., 2012). TCs act to naturally cool the oceans and atmosphere in tropical latitudes by transporting heat to higher latitudes (Emanuel, 1987). Thus, we can expect that TC behavior, including intensity, may vary in a warmer climate (Hall et al., 2021; Knutson et al., 2015, 2019; Kossin, 2017; Lin et al., 2010; Seneviratne et al., 2021; Villarini & Vecchi, 2013). However, uncertainty remains about how other characteristics of TCs, including their genesis, tracks, and termination, may change (Chu et al., 2020; Colbert et al., 2013; Daloz et al., 2015; Garner et al., 2017; Hall et al., 2021; Kossin et al., 2010).

Here, we use >35,000 synthetic TCs downscaled from three Coupled Model Intercomparison Project version 5 (CMIP5) global climate models (GCMs) to investigate changes to the characteristics of North Atlantic TC tracks that impact two major cities (New York City (NYC) and Boston, MA, USA) and the largest naval complex in the world (Norfolk, VA, USA; U.S. Navy, 2020) in three distinct climatological eras (pre-industrial, modern, and future). To gain a long-term perspective of how TC tracks and key characteristics along those tracks vary in a warming climate, we consider changes to (a) TC genesis, tracks, and termination in the North Atlantic and (b) location and magnitude of TC minimum translation speeds from the past millennium through the end of the 21st century for a strongly forced climate scenario (RCP8.5). In what we believe is the first long-term study of its kind, we evaluate the implications of these changes to TC tracks for several specific locations—NYC, Boston, and Norfolk—all of which are key points of interest that are susceptible to TC hazards.

## 2. Results

We investigate changes to key characteristics of TC trajectories from the pre-industrial (850–1800 CE) to modern (1970–2005 CE) to future (2080–2100 CE) eras for three different GCMs (MPI, CCSM4, and IPSL; see Section 4). Characteristics considered include: (a) locations of TC genesis, tracks, and termination in the North Atlantic; and (b) locations and magnitudes of TC minimum translation speed. In some cases, we find persistent, monotonic trends in changing TC track characteristics (e.g., location of TC genesis and minimum translation speed), while in other cases we find nonmonotonic trends across time (e.g., location of TC termination, and proximity of storms to NYC; Figures 1 and 2 and Table 1). We note that in most cases where trends of our model ensemble for TC characteristics are nonmonotonic across time, there is overlap in error bars of changes between the pre-industrial and modern eras (Figures 2a–2c and Table 1), and that such nonmonotonic trends tend to occur primarily in instances where there is significant variability across individual models in terms of changing track characteristics from the pre-industrial to modern eras.

### 2.1. Tropical Cyclone Genesis, Tracks, and Termination in the North Atlantic

#### 2.1.1. Tropical Cyclone Genesis

From the pre-industrial to the end of the 21st century, there is a decreasing density of TC genesis in the North Atlantic main development region (MDR; defined here as the region from 6°–18°N to 20°–60°W; Figure 1), and an increasing density of TC genesis in regions that include the Caribbean and waters just offshore of the U.S. southeast coast (Figures 1a and 1b). These trends are evident not only for the full ensemble, but also in all individual models (Figures 1a, 1b, 2a and 3; Figure S1 in Supporting Information S1).

Across the model ensemble, there is a consistent increase ($p = 0.01$) in the likelihood of storms forming along the U.S. southeast coast (defined as the region from 25°–37°N and 45°–85°W; Figures 1a and 1b), and a consistent decrease ($p = 0.01$) in the probability of storms forming in the MDR from the pre-industrial era to the end of the 21st century (Figure 2a and Table 1). These results hold for individual models, with the sole exception that the increase in genesis along the U.S. southeast coast is not significant from the pre-industrial to the modern era in the MPI model (Figure 2a).

The analysis of environmental variables from the GCMs used to generate TC tracks suggests that changes to TC genesis locations may be influenced by variations of both relative humidity and vertical shear. From the pre-industrial to the modern era, shear increases in the MDR, causing less favorable genesis conditions (e.g., Camargo et al., 2007) in the region over this time (Figure S2 in Supporting Information S1). Though shear appears less likely to be a factor in genesis changes from the modern era to the future, decreased relative humidity in the MDR over this time may cause the region to become less conducive to TC genesis by 2100 CE (Figure S2 in Supporting Information S1).

#### 2.1.2. Tropical Cyclone Tracks

By the end of the 21st century, the density of TC tracks traveling close to NYC decreases compared to the modern era, with TCs tending instead to remain offshore at their nearest approach to NYC (Figures 1d and 3; Figures S3 and S4 in Supporting Information S1). Across our model ensemble, the proportion of TCs remaining 150 km or farther away from NYC increases by the end of the century ($p = 0.01$; Figures 1d and 2b and Table 1); this trend is present within both CCSM4 and IPSL models but is only significant ($p = 0.01$) for the IPSL model (Figure 2b). In the MPI model, by contrast, there is a slight increase in the number of TCs traveling within 75 km of NYC and a decrease in the number of storms remaining at least 150 km away from NYC. This is likely due to a split in the location where TC tracks make their nearest

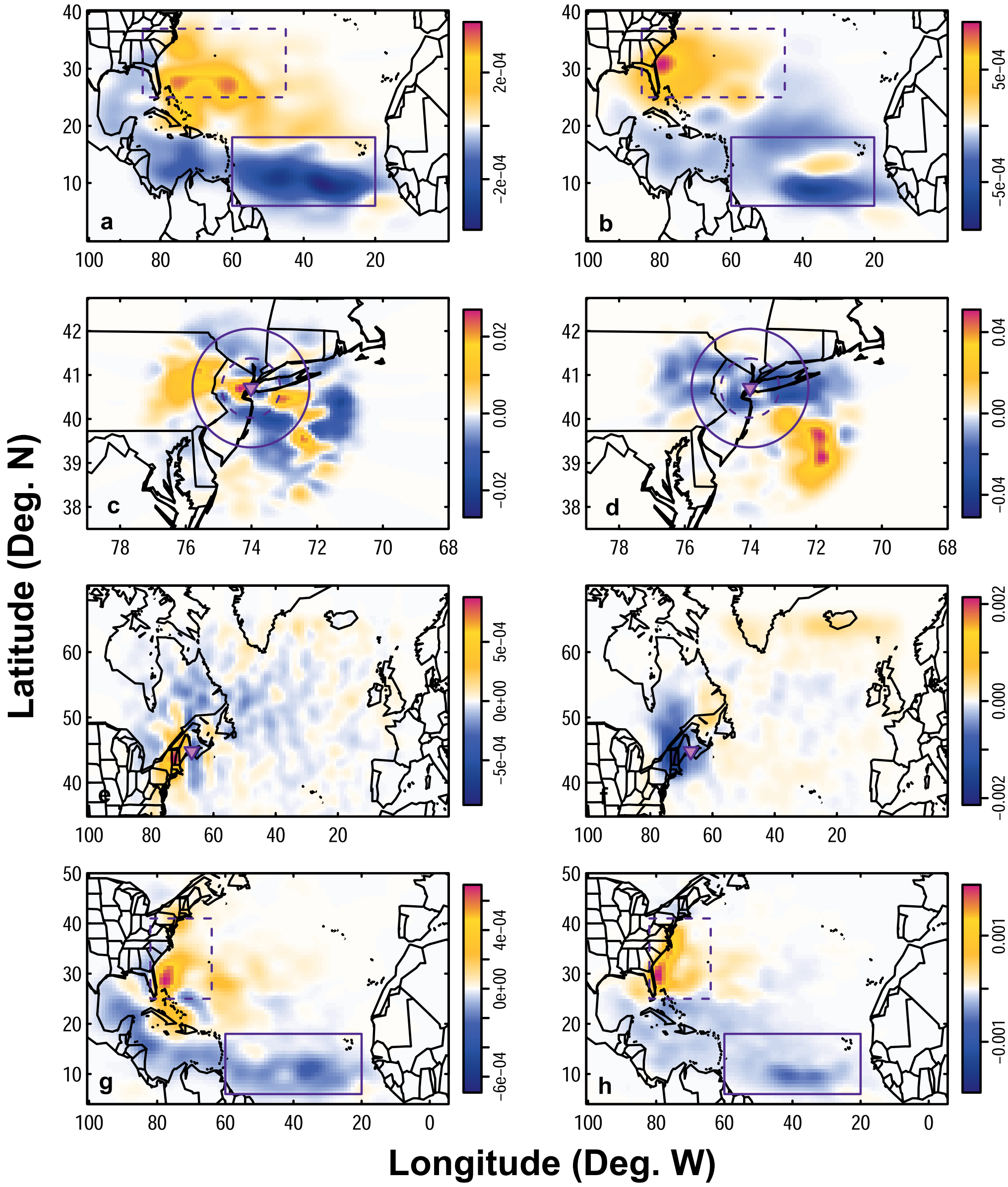


**Figure 1. Density difference maps of TC characteristics.** Maps of the density differences of (a) TC genesis points (modern vs. pre-industrial). (b) TC genesis points (future vs. modern). (c) TC nearest point to the Battery (modern vs. preindustrial). (d) TC nearest point to the Battery (future vs. modern). (e) TC termination points (modern vs. pre-industrial). (f) TC termination points (future vs. modern). (g) Location of TC minimum translation speed (modern vs. pre-industrial). (h) Location of TC minimum translation speed (future vs. modern). Also shown are: (a and b) Location of MDR (solid rectangle) and U.S. Southeast Coastal region (dashed rectangle); (c and d) Location of The Battery, NYC (purple triangle); circles showing the 75 km (dashed) and 150 km (solid) distance from the Battery; (e and f) Location of West Quoddy Head Maine, most eastern point in United States (purple triangle); (g and h) Location of MDR (solid rectangle) and U.S. East Coast Region (dashed rectangle).

approach to the city in the MPI model, with increases both in the number of tracks remaining offshore and in the number of tracks traveling west of the city, where they often remain within 150 km of NYC (Figure S4 in Supporting Information S1).

Despite some variation in the probability of storms remaining 150 km or farther away from NYC, all models suggest increases from the modern to the future in the density of TC tracks remaining offshore in a region southeast of NYC at their nearest approach to the city (Figure 1d and Figure S4 in Supporting Information S1).

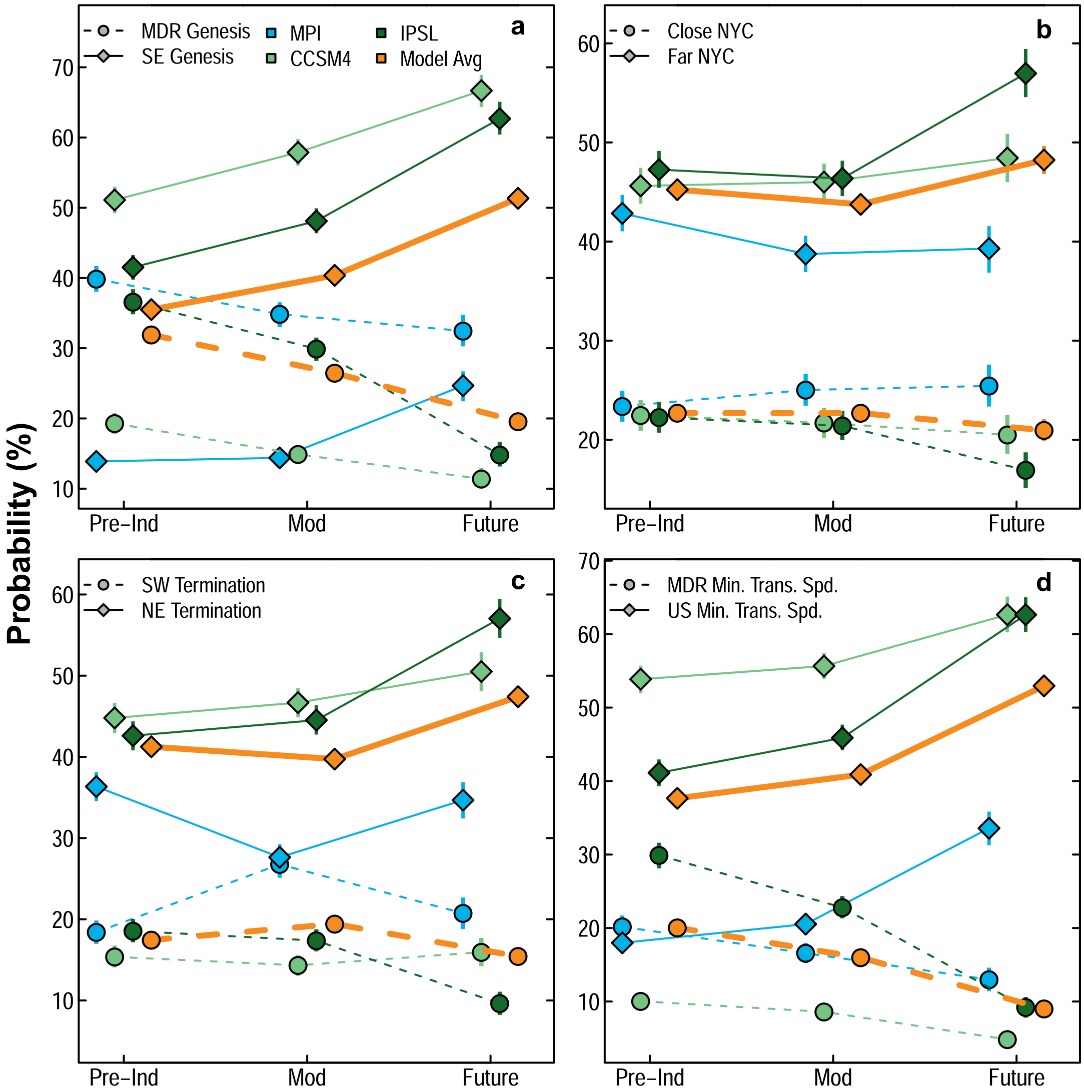


**Figure 2. Probabilities of TC track characteristics.** Probability of (a) TC genesis occurring in the MDR (MDR Genesis) or along the United States Southeast Coast (SE Genesis). (b) TC nearest point to The Battery being ≤75 km (Close NYC) or ≥150 km (Far NYC). (c) TC termination occurring southwest (SW Termination) or northeast (NE Termination) of West of West Quoddy Head, ME. (d) Probability of TC minimum translation speed occurring in the MDR (MDR Min. Trans. Spd.), or along the United States East Coast (US Min. Trans. Spd.). Error bars show the bootstrapped 99% credible intervals. Note that Figure 1 shows key locations and regions including The Battery; West Quoddy Head, ME; the MDR; the United States Southeast Coast region; and U.S. East Coast region.

Similar increases in this region can be seen in the CCSM4 and IPSL model from the pre-industrial to the modern era (Figure S4 in Supporting Information S1).

There is some indication that the changing proximity of TC tracks to NYC may be influenced by variations in vertical shear. For example, there is a greater decrease in vertical shear for TCs that remain at least 150 km away from NYC than for TCs that travel within 75 km of NYC over the modern to future eras (Figure S5 in Supporting Information S1). This result is consistent with a Principal Component Analysis (PCA) performed for environmental variables (Table S1 in Supporting Information S1).

### 2.1.3. Tropical Cyclone Termination

There are significant changes in where TCs terminate by the end of the 21st century compared to the modern era. By 2080–2100 CE, there is a decrease in the density of TCs terminating near New England, and an

**Table 1**
*Percentages of Tropical Cyclone Tracks With Given Characteristics in Each Time Period*

| | | Pre-industrial | Modern | Future |
|---|---|---|---|---|
| Proximity to NYC | ≤75 km | 22.7% (21.8%–23.6%) | 22.7% (21.8%–23.6%) | 21.0% (19.9%–22.1%) |
| | ≥150 km | 45.2% (44.1%–46.2%) | 43.8% (42.7%–44.8%) | 48.2% (46.8%–49.7%) |
| Genesis point | MDR | 31.9% (30.9%–32.9%) | 26.5% (25.6%–27.4%) | 19.6% (18.4%–20.7%) |
| | SE coast | 35.5% (34.5%–36.5%) | 40.4% (39.4%–41.5%) | 51.3% (49.9%–52.8%) |
| Termination point | SW West Quoddy Head, ME | 17.4% (16.6%–18.3%) | 19.4% (18.6%–20.3%) | 15.4% (14.5%–16.4%) |
| | NE West Quoddy Head, ME | 41.2% (40.2%–42.3%) | 39.7% (38.7%–40.8%) | 47.4% (46.1%–48.7%) |
| Minimum translation speed | MDR | 20.0% (19.2%–20.9%) | 16.0% (15.2%–16.8%) | 9.0% (8.2%–9.8%) |
| | US coast | 37.7% (36.6%–38.7%) | 40.9% (39.8%–41.9%) | 53.0% (51.5%–54.3%) |

*Note*. Bootstrapped 99% credible intervals are shown in parentheses; categories are the same as those shown in Figure 2.

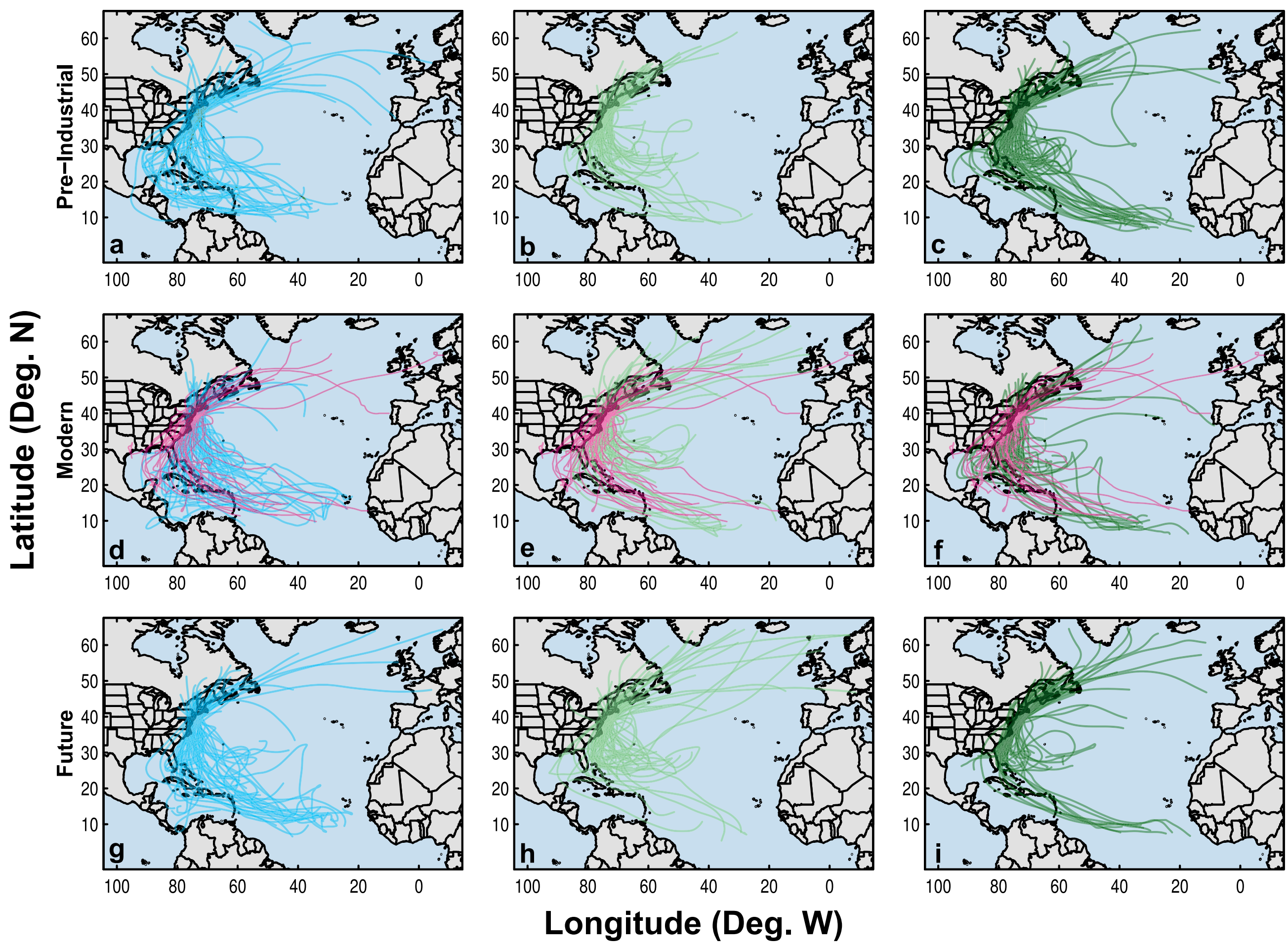


**Figure 3. Tropical Cyclone Tracks.** Random samples of 50 TC tracks from (a, d, and g) The MPI model (Column 1, blue); (b, e, and h) The CCSM4 model (Column 2, light green); (c, f, and i) The IPSL model (Column 3, dark green) for the pre-industrial era (Row 1), modern era (Row 2), and future (Row 3). Also shown are tracks of historical Atlantic tropical cyclones that traveled within 250 km of NYC (d–f; pink). Observed tracks are from the National Oceanic and Atmospheric Administration's HURDAT2 Best Track database (Landsea & Franklin, 2013).

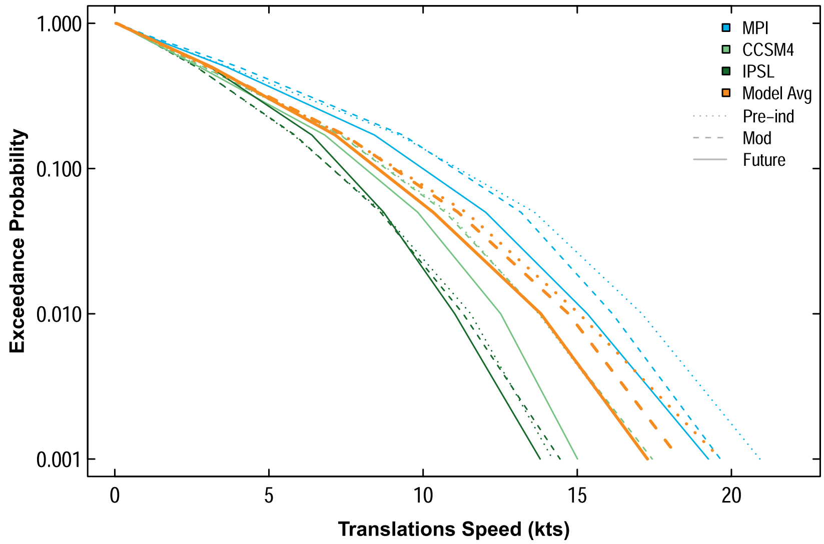


**Figure 4. Exceedance Probabilities of TC Minimum Translation Speeds.** Survival functions showing exceedance probabilities of lifetime minimum translation speeds of TCs during the preindustrial era (dotted lines), the modern era (dashed lines), and the future era (solid lines). Models/ensemble are indicated by color, as in Figure 2.

increase in the density of TCs terminating north and east of the U.S. Atlantic coast (Figures 1f and 3; Figure S6 in Supporting Information S1).

From the modern to the future era, more TCs in our model ensemble terminate at locations northeast of West Quoddy Head, ME (44.8°N–67.0°W), which is the eastern-most point of the U.S (Figures 1e, 1f and 2c and Table 1). Likewise, fewer TCs terminate southwest of this location over the same period ($p$ = 0.01; Figure 2c and Table 1). These results generally hold for individual models, with a few exceptions from the CCSM4 model, where increases in termination northeast of West Quoddy Head are not significant and there is an apparent (though not significant) increase in termination southwest of this location over this time (Figure 2c).

By the end of the 21st century, a greater proportion of TCs are sustained until they reach the latitude of 65°N (at which point TCs are automatically terminated; see Section 4) than in the modern or pre-industrial eras (Figures 1e and 1f). This result is consistent across all models (Figure S6 in Supporting Information S1).

### 2.2. Location and Magnitude of Tropical Cyclone Minimum Translation Speeds

From the pre-industrial era through the end of the 21st century, there is a persistent change in the locations at which TCs reach their minimum translation speed (i.e., their slowest forward motion)—a noteworthy track variation, given that slower-moving storms have a greater potential to inflict damages along their paths. Over this period, across all models, there are decreases in the density of TCs with minimum translation speeds in the MDR and western Gulf of Mexico and increases in the density of TCs with minimum translation speeds in the Caribbean and along the U.S. Atlantic coast (Figures 1g and 1h; Figure S7 in Supporting Information S1). As time progresses, a greater proportion of TCs in the full ensemble move forward most slowly in a region along the U.S. Atlantic coast (25°–41°N and 64°–82°W; $p$ = 0.01; Figures 1g and 1h), and a smaller proportion of TCs move most slowly in the MDR ($p$ = 0.01; Figure 2d and Table 1). These results generally hold for individual models as well, though shifts from the pre-industrial to the modern era are not significant for the MPI and CCSM4 models (Figure 2d).

There are also decreases in minimum translation speed distributions from the pre-industrial era to the end of the century (Figure 4). Given that the slowest minimum translation speeds in all time periods approach a limit of 0 kts, decreases in TC forward motion over time are most notable for the central and upper portions of the minimum translation speed distributions. This decrease suggests that more TCs may not only reach

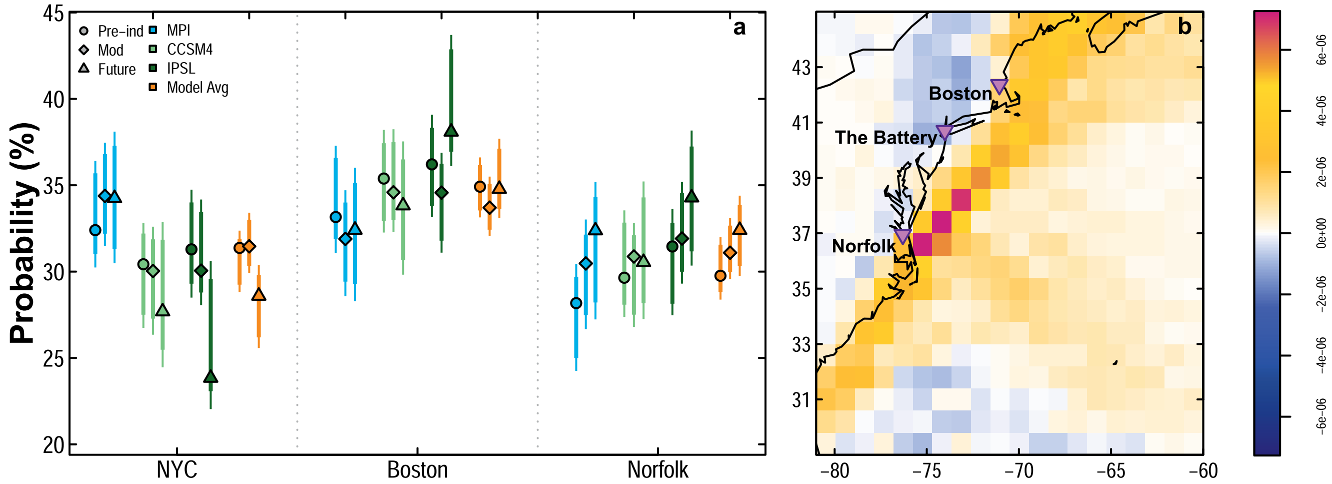


**Figure 5. Probability of TCs passing within 100 km of various points of interest.** (a) Probability (points), 95% (thick bars), and 99% (thin bars) credible intervals of TCs passing within 100 km of The Battery in NYC, NY, USA; Boston, MA, USA; and Norfolk, VA, USA during each time period. (b) Gridded density differences of TC tracks across all models from 2080 to 2100 compared to the modern era.

their slowest speeds along the U.S. Atlantic coast in the future, but that some future minimum translation speeds may also be slower than they have been in the past.

Changing locations of minimum translation speed are not well-explained by changes to temperature, relative humidity, or vertical shear within our data sets. Though there are some shifts in these environmental variables that coincide with minimum translation speed points over time (Figure S8 in Supporting Information S1), no clear trend emerges to sufficiently explain the spatial changes in minimum translation speeds. However, an examination of 850 hPa environmental wind speeds at the time of minimum translation speed show a slight shift in average environmental wind direction over time, with frequency of WSW wind directions decreasing and WNW wind directions increasing from the pre-industrial to the future (Figure S9 in Supporting Information S1). The magnitude of environmental wind speeds also slow over this time period (Figure S9 in Supporting Information S1). Such variations in environmental winds could impact storm minimum translation speed, as both direction and magnitude signal potentially less effective steering currents for storms along their typical paths.

## 2.3. Implications of Changing Tropical Cyclone Tracks for Key Locations on the U.S. East Coast

### 2.3.1. Variations in Tropical Cyclone Track Proximity

In future simulations, there is an increased tendency for TCs to remain offshore at their nearest approach to NYC (Figures 1d and 3; Figures S3 and S4 in Supporting Information S1), rather than making landfall. By the end of the 21st century it also becomes more likely within our model ensemble ($p = 0.01$) that TCs will travel within 100 km of Boston, MA, USA and/or Norfolk, VA, USA than within 100 km of NYC (Figure 5). From the pre-industrial era to the end of the 21st century, the likelihood of TCs traveling within 100 km of Boston remains relatively constant, the likelihood of TCs traveling within 100 km of Norfolk increases, and the likelihood of TCs traveling within 100 km of NYC decreases. These changes combine to make it more likely that any given TC will travel within 100 km of Boston ($p = 0.01$) and/or Norfolk ($p = 0.05$) than that the TC will travel within this distance of NYC.

Within individual models, trends in TC proximity to NYC, Boston, and Norfolk are generally consistent across both the CCSM4 model and the IPSL models, with the most significant shifts occurring in the IPSL model (Figure 5). Consistent with our model ensemble results, the MPI model indicates an increase through time in the number of TCs traveling within 100 km of Norfolk; however, there are also slight increases in the numbers of TCs traveling near NYC, due to an increase in tracks traversing inland.

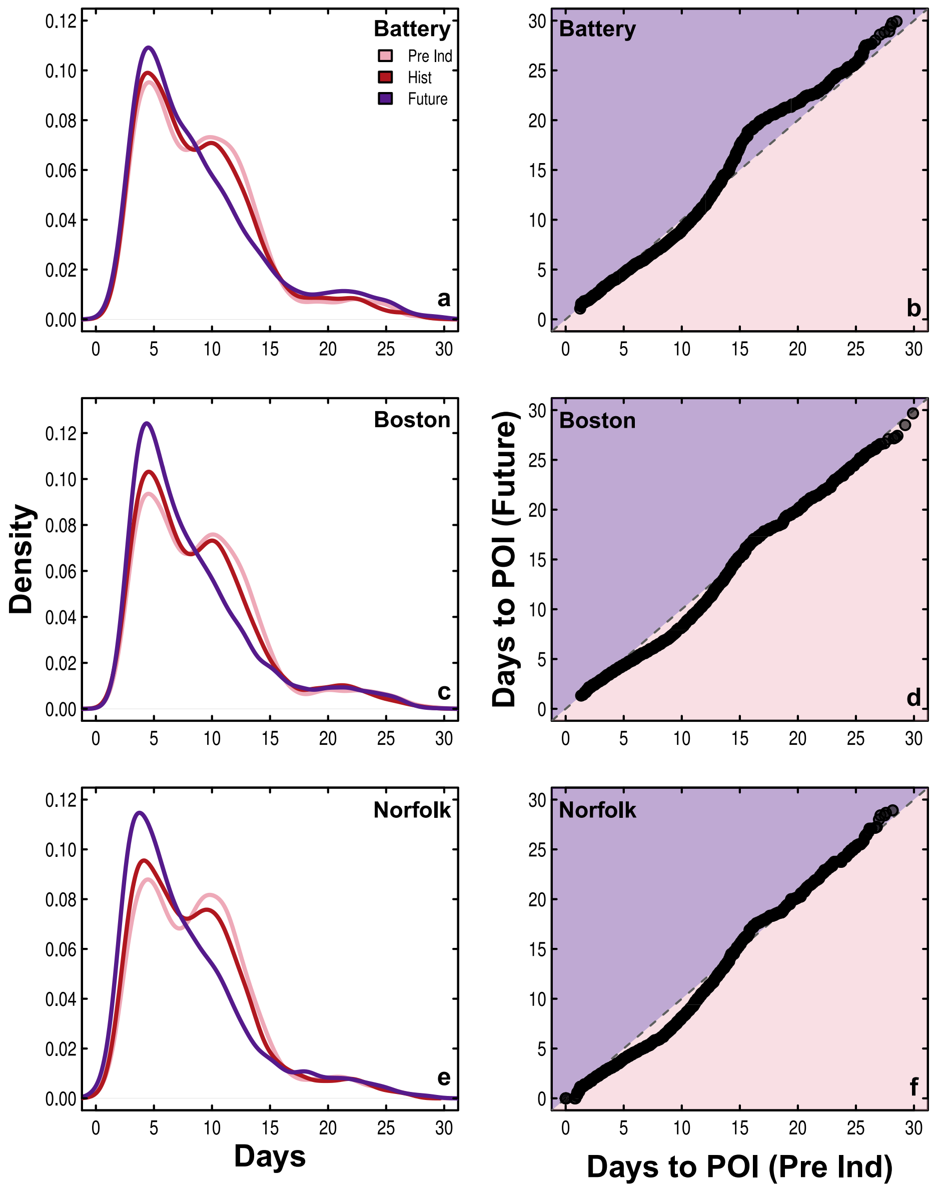


**Figure 6. Time from genesis to points of interest.** Probability density functions (a, c, and e) and QQ-plots (b, d, and f) of the time in days from when TCs form until when they within 100 km of (a and b) The Battery (NYC), (c and d) Boston, MA, USA and (e and f) Norfolk, VA, USA. Probability density functions are shown for the pre-industrial, modern, and future time periods. QQ plots show the difference in quantiles of distributions from the pre-industrial (pink) and future (purple) eras. Gray dashed lines on the QQ-plots show the one-to-one line; when points deviate from the line, the pre-industrial and future distributions are significantly different.

#### 2.3.2. Consequences of Tropical Cyclone Track Variations for Communities Along the U.S. Atlantic Coast

From the pre-industrial era through the end of the 21st century, the time from genesis until the TC comes within 100 km of NYC, Boston, or Norfolk decreases significantly, with the largest decreases occurring in Norfolk (Figure 6). For all three cities, distributions of the number of days from TC formation until the TCs travel within 100 km of the location are bimodal in the pre-industrial and modern eras, with substantial numbers of TCs forming in both the Caribbean and along the U.S. southeast coast (first peak, less than a week to reach each city) and the MDR (second peak, 1.5–2 weeks to reach each city). By the end of the 21st century, distributions are unimodal, with a single peak at approximately 5 days, representing an increased number of TCs forming closer to the U.S. southeast coast, though each distribution retains a long upper tail (Figures 1a, 1b, 3, 6a, 6c and 6e). When considering storms that reach NYC, Boston, or Norfolk in under 14 days, the time from genesis until the TC comes within 100 km of the city significantly decreases from the pre-industrial to the future (Figures 6b, 6d and 6f).

From the pre-industrial to the end of the 21st century, NYC, Boston, and Norfolk also all experience increases in the duration of TC impacts due to a combination of slower TC translation speeds (Figure 4 and Figure S10 in Supporting Information S1) and variations in TC tracks (Figure 5). Here, we define TC impacts to be occurring for a city any time that the city is contained within the TC's radius of maximum winds. Though there are no major shifts in the peaks of the distributions that describe the average number of hours TCs impact each location across time periods, all of the distributions exhibit long, risk-determining tails (Figures 7a, 7c and 7e). Our comparison of these longest-lasting events reveals significantly longer duration of impacts for all three cities by the end of the 21st century compared to the pre-industrial era (Figures 7b, 7d and 7f). Consistent with shifts in the location of TC minimum translation speed over this time, increases in the duration of TC impacts are greatest at Norfolk, where the longest lasting future storms often persist about twice as long as their pre-industrial counterparts (Figure 7f).

## 3. Discussion

Changing TC characteristics near the U.S. Atlantic coast have important consequences for the hazards that this highly populated region faces in a warming climate (Emanuel, 2005; Garner et al., 2017; Grinsted et al., 2019; Lin et al., 2016; Pielke, 2007). To fully appreciate how TC hazards may evolve, it is necessary understand how both TC tracks and characteristics may vary. Previous studies have focused on how varying environmental conditions may impact TC intensity, size, or flood potential for the U.S. Atlantic coast (Lin et al., 2012; Marsooli et al., 2019; Ting et al., 2019). Other studies specifically investigated changing TC tracks for the modern or future eras (Colbert et al., 2013; Hall et al., 2021). Our work adds to these previous studies by providing a long-term perspective of TC track variations from the pre-industrial era to the end of the 21st century, including an assessment of how such variations may impact the TC hazard facing key locations along the U.S. Atlantic coast.

Environmental requirements for TC genesis include adequately warm ocean temperatures, low wind shear, sufficient humidity levels, ample Coriolis force from Earth's rotation, and a pre-existing low-level disturbance from which the TC may begin to develop (Camargo et al., 2014; Gray, 1975). The North Atlantic MDR, located along the northern edge of the Intertropical Convergence Zone (ITCZ), is an area in which it is common for these conditions to be met and in which it is thus common for TCs to form. Our results, however, suggest that from the pre-industrial era to the end of the 21st century under RCP8.5, it becomes more likely that TCs impacting the northeastern U.S. will form closer to U.S. coastlines, in an area just offshore of the U.S. southeast coast. It becomes correspondingly less likely that such TCs will form in the MDR. An increase in TC formation near U.S. coastlines could limit lead time before storm impacts are felt along U.S. coastlines, escalating forecasting challenges (Halperin et al., 2017) and amplifying hazards in coastal communities.

Long-term variations in TC genesis locations support previous paleotempestology work pertaining to the influence of ITCZ meridional shifts on TC activity in the North Atlantic (Broccoli et al., 2006; Van Hengstum et al., 2016). Geologic records suggest an elevated level of TC activity along the western North Atlantic margin from 2500 to 1000 yr ago, when the ITCZ was located at higher latitudes (Van Hengstum et al., 2016). It is reasonable to anticipate that this region could see increased TC activity in the future with another migration of the ITCZ (Burnett et al., 2021; Van Hengstum et al., 2016). Given that variation in the ITCZ position is driven partially by differential heating and cooling of the hemispheres (Broccoli et al., 2006), and given the amplified warming of the northern hemisphere relative to the southern hemisphere in a warming climate (Stocker et al., 2013), it is plausible that a northward shift in the ITCZ could help drive increased density of TC genesis along the U.S. southeast coast in the future.

As TC genesis locations evolve, there are also variations in the proximity of TC tracks to U.S. coastal communities. Previous studies postulated an easterly TC track shift near NYC from the modern to the future as the cause of minimal changes to overall storm surge heights despite potentially stronger storms by the end

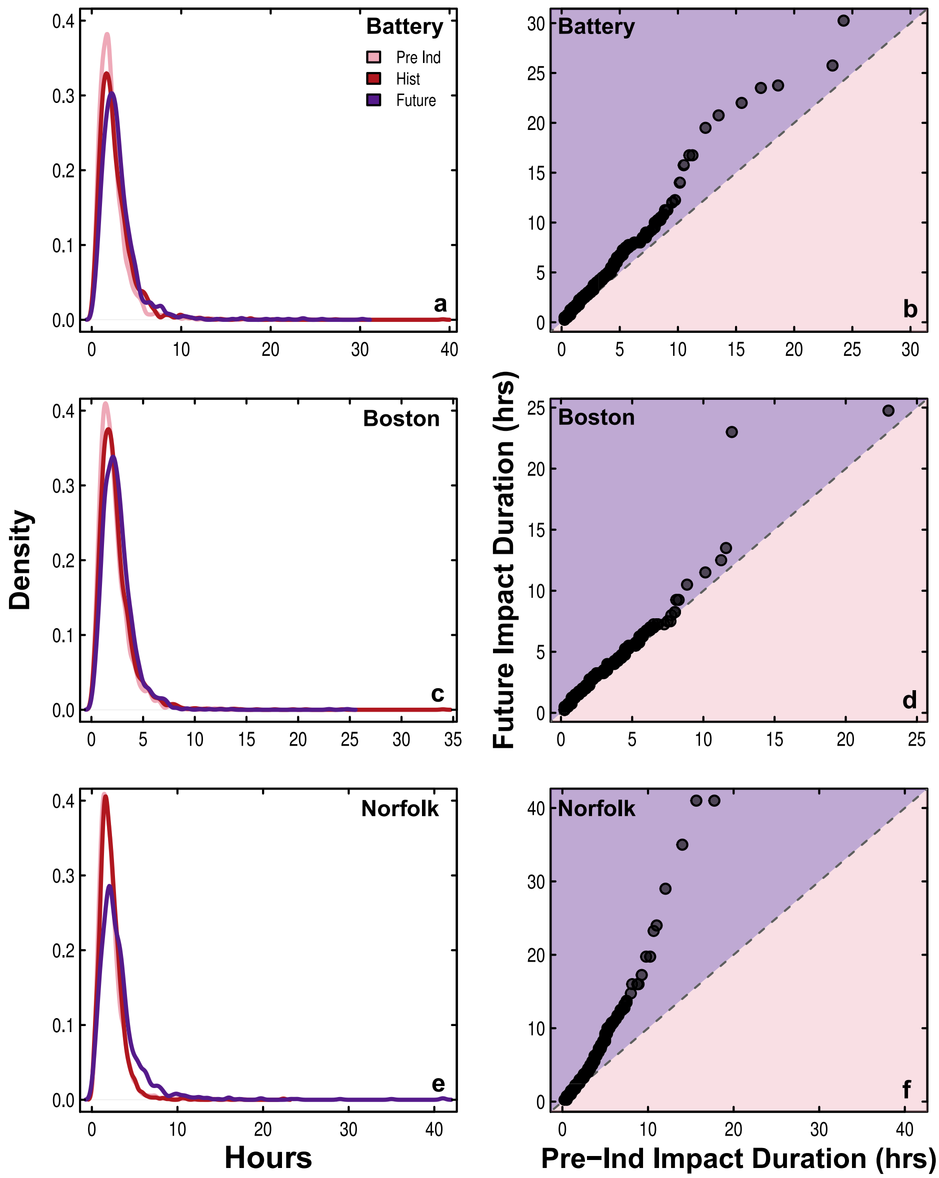


**Figure 7. Duration of TC impacts at points of interest.** Probability density functions (a, c, and e) and QQ-plots (b, d, and f) of the duration (hrs) of TC impacts at (a and b) The Battery (NYC), (c and d) Boston, MA, USA and (e and f) Norfolk, VA, USA. Probability density functions are shown for the pre-industrial, modern, and future time periods. QQ plots show the difference in quantiles of distributions from the pre-industrial (pink) and future (purple) eras. Gray dashed lines on the QQ-plots show the one-to-one line; when points deviate from the line, the pre-industrial and future distributions are significantly different.

of the century (Garner et al., 2017). Here, we find that compared to the modern era, TC tracks become farther removed from NYC in the future under a high-emissions scenario—a finding that is consistent with the suggested track shift in Garner et al. (2017), which was suggested not only for the MPI, CCSM4, and IPSL models, but also for the HadGEM, GDL, MRI, and MIROC submissions to CMIP5 (see Garner et al., 2017; Figure S7 in Supporting Information S1). Although such a track shift may benefit NYC, other communities do not see the same advantage. For example, there is no change in TC proximity to Boston during the 21st century, resulting in a greater likelihood that storms will pass within 100 km of Boston than NYC by the year 2100, which causes a varying TC hazard for these two major coastal cities that are only about 300 km apart. By the end of the century, it also becomes more likely that TCs will travel within 100 km of Norfolk than NYC. This suggests an increasing TC hazard for Norfolk relative to NYC, which could translate to national security risks for the U.S. (National Research Council, 2013: Committee on Assessing the Impact of Climate Change on Social and Political Stresses), given the significant military infrastructure housed in Norfolk. Such modifications of TC track proximity to coastal communities are consistent with recent observational studies (Wang & Toumi, 2021). Furthermore, we find that the evolution of genesis points combined with track variations causes all three cities (NYC, Boston, and Norfolk) to experience decreases in the time between when TCs form and when they approach the city, reducing the time available for these coastal communities to prepare for TC events. These results emphasize the necessity and urgency of adaptation and mitigation measures to help protect coastal communities both now and in the future.

Changes to translation speeds combined with shifts in TC tracks further complicate the evolving hazard to North Atlantic coastlines. From the pre-industrial to the end of the 21st century, we find that more TCs reach their slowest speeds along the U.S. Atlantic coast than in the MDR. Furthermore, consistent with previous studies (Kossin, 2018; Zhang et al., 2020), overall magnitudes of storm minimum translation speeds decrease (Figure 4). These variations in translation speed combined with changing storm tracks result in significant increases from the pre-industrial era to the end of the 21st century in the average amount of time that TCs impact NYC, Boston, and Norfolk. These results for U.S. Atlantic coastal communities are particularly concerning, given that slow-moving TCs have an increased potential to inflict damages in the regions through which they travel. For instance, such TCs may produce long-lived storm surges, increasing the probability of storm surge occurring simultaneously with astronomical high tide, and leading to enhanced overall flood heights (Kemp & Horton, 2013; Reed, Mann, Emanuel, Lin, et al., 2015). For example, slow-moving Hurricane Dorian (2019) produced inundation levels of up to 6 m above ground level due to combined tide and storm surge in portions of the Bahamas (Avila et al., 2020). Moreover, there is medium-to-high confidence that TC precipitation rates will increase in a warmer climate (Knutson et al., 2019), and slow-traveling TCs magnify the potential for catastrophic rainfall events (Kossin, 2018; Lai et al., 2020). For example, Hurricane Harvey stalled over Texas in 2017, producing >60″ of rain in some areas, and becoming the most significant TC rainfall event in U.S. history (Blake & Zelinsky, 2017). Such rainfall events have the potential not only to create extreme inland flooding, but also to generate compound flood events at coastlines as rainfall totals amplify flooding associated with storm surge (Wahl et al., 2015).

Though we investigated changes to vertical wind shear and humidity that may contribute to evolving TC tracks in the North Atlantic, recent studies also suggest other possible drivers for varying TC track characteristics (Chu et al., 2020; Daloz et al., 2015; Knutson et al., 2019; Kossin et al., 2014, 2016; Nakamura et al., 2017; Wang & Toumi, 2021). For example, northerly shifts in TC genesis and termination that we identify are consistent with a poleward expansion of the tropics, which has been linked to anthropogenic warming (Kossin et al., 2016; Lucas et al., 2014; Nakamura et al., 2017). Other studies have suggested that zonal changes in environmental steering flow may play a role in a westward shift in TC tracks globally (Wang & Toumi, 2021), which may include changes that we find in genesis and the proximity of storms to locations such as Norfolk. Finally, some studies have emphasized a connection between increasing sea-surface temperatures (SSTs) and heightened spatial density of TCs, especially in regions where SSTs increase relatively more than other areas (Murakami et al., 2012). Shifting densities of TC tracks identified here align with the projected increases of SSTs within CMIP5 models under RCP8.5 for the North Atlantic as a whole, and the U.S. shelf in particular (Alexander et al., 2018), indicating that rising SSTs may also be an important driving factor.

In a warming climate, we expect changes to a variety of TC characteristics, including their intensity, size, and flood hazard (Knutson et al., 2019). Our results illustrate the importance of considering not only such metrics that characterize a TC, but also the necessity of understanding how changing TC trajectories may impact the regions where TCs start, travel, end, and move most slowly. Such characteristics play a vital role in determining the overall hazard coastlines face from TCs both now and in the future. Finally, it is imperative that we understand the mechanisms that drive changes to TC tracks in a warming climate. We identify several factors that support the track shifts found here and elsewhere in the literature. However, additional studies, including analyses of larger model ensembles, are warranted to (a) reduce uncertainty; (b) better understand the changes between "modern" and "future" periods, including the magnitude of future changes under different emission scenarios; and (c) clarify the precise environmental processes driving modifications to TC tracks, given the potential of such variations to drastically impact the hazards facing our coastal communities in a changing climate.

## 4. Methods

### 4.1. Synthetic Tropical Cyclones

Although past investigations have considered changes to TC tracks in the North Atlantic in a warming climate (e.g., Colbert et al., 2013; Hall et al., 2021; Kossin et al., 2010), such studies are sometimes limited in scope, focusing either on the relatively short and potentially biased observational record of TCs in the North Atlantic (e.g., Kozar et al., 2013; Reed, Mann, Emanuel, & Titley, 2015), future TCs, or some combination of these. To overcome this limitation, we use synthetic TCs downscaled from GCMs for our study. Using the statistical/deterministic model described in Emanuel et al. (2006, 2008), we generate large numbers of synthetic TCs under various climate scenarios which are ideal for assessing long-term TC activity under plausible past climate scenarios, as well as under future warming. Downscaled TCs are generated using a combination of thermodynamic and kinematic state variables from CMIP5 GCMs (Taylor et al., 2012).

Downscaled TCs are generated using a random seeding process (Emanuel et al., 2008). In this approach, warm-core vortices with peak wind speeds of only 12 m/s and almost no midlevel humidity anomaly in their cores are distributed throughout the Atlantic basin everywhere north of 2° latitude and at all times of the year. Most of these vortices fail to develop into TCs, due to unfavorable environmental conditions, such as low potential intensity or large wind shear. However, if the vortices develop winds of at least 21 m/s (40 kts), they are considered to have formed a TC (Emanuel et al., 2008), and are included in our downscaled tracks. The first point at which a vortex becomes a TC is considered the genesis point for the storm.

A beta-and-advection model is used to approximate TC tracks, which incorporates the 850 and 250 hPa wind fields from the GCMs to articulate storm motion (Emanuel et al., 2008). As detailed in Emanuel et al. (2008), the beta-and-advection model represents the 850 and 250-hPa wind fields as Fourier series of random phase constrained to have monthly means, variances, and covariances calculated from daily data, and to have a geostrophic turbulence power-law distribution of kinetic energy. A comparison of simulated tracks during the modern era and observed tracks from the National Oceanic and Atmospheric Administration's HURDAT2 Best Track database (Landsea & Franklin, 2013) occurring since 1970 reveals that simulated TC track patterns are consistent with observed patterns (Figure 3).

Environmental variables associated with each storm are taken directly from GCM fields that describe the 600 hPa relative humidity, 600 hPa atmospheric temperature, and 850–250 hPa vertical wind shear of the environment in which each storm is located. These values thus provide a snapshot of the state of the atmosphere that aligns in time and space with the location of each storm at each 2-hr point along every track.

We focus on TCs generated from three CMIP5 (Taylor et al., 2012) models (Max Planck Institute for Meteorology [MPI], Community Climate System Model version 4 [CCSM4], and Institut Pierre Simon Laplace [IPSL]), with TCs filtered to travel within 250 km of NYC, as in Garner et al. (2017). The use of the MPI, CCSM4, and IPSL models allows us to more thoroughly investigate the long-term implications of shifting TC tracks near NYC originally suggested in Garner et al. (2017), though we note that future studies to consider and compare similar track variations that may exist in CMIP6 models would also be useful. The MPI, CCSM4, and IPSL models are the only models used in Garner et al. (2017) that contain the variables necessary to downscale TCs for the pre-industrial, modern, and future time periods—all three of which are necessary to establish historical context for present and future changes to TC tracks in the Atlantic. We define these time periods as follows:

1. **The pre-industrial era (850–1800 CE):** Climatological conditions prior to major anthropogenic influence.
2. **The modern era (1970–2005 CE):** Recent climatological conditions.
3. **The future era (2080–2100 CE):** Climatological conditions under additional warming due to anthropogenic greenhouse gas emissions. TCs are generated for a very high-emissions scenario (Representative Concentration Pathway 8.5; RCP8.5), which we expect to provide an upper bound on potential changes to future TC tracks (Riahi et al., 2011). We focus on a strongly forced future in order to maximize the

potential signal; under more realistic emissions scenarios (Hausfather & Peters, 2020), we may expect to see changes smaller than those simulated here.

Pre-industrial and modern simulations each contain ~5,000 TCs per model, while future simulations for the RCP8.5 scenario include >12,000 TCs per century, or nearly 3,000 TCs per model during the 2080–2100 time period that we focus on at the end of the 21st century. These large numbers of TCs allow us to perform meaningful statistical analyses of changing TC characteristics over long time periods. Overall TC frequency is determined by calculating the ratio of total simulated TCs to the total number of TCs seeded (Emanuel et al., 2008).

Since TCs are filtered to travel within 250 km of The Battery in NYC, it should be noted that the results presented here are not necessarily representative of basin-wide storm behavior in the North Atlantic, but are highly relevant for the subset of TCs that impact the densely populated northeastern coastline of the U.S. Furthermore, many of the downscaled TCs follow paths that bring them near to other points of interest along the U.S. Atlantic coast, including Boston, MA, USA and Norfolk, VA, USA. During the three time periods considered, we find that 34% of TCs travel within 100 km of Boston and 31% travel within 100 km of Norfolk—percentages that are similar to the number of TCs that come within this distance of NYC (31%).

TC tracks are considered to end when one of three conditions is met: storm maximum winds fall below 13 m/s, the storm has existed more than 30 days, or the storm travels outside of a pre-defined latitude/longitude box (4°–65°N and 0°–110°W). Because of the third constraint, there can be challenges to fully assessing changes to the region in which TCs terminate, as TCs will be prevented from traveling farther north than 65°N, or farther east than 0° (Figures 1e and 1f); however, it is nonetheless useful to assess the locations of TC track termination over time, to see if there are broad changes to where TCs dissipate, including potential increases in the number of tracks that reach the latitude/longitude boundary.

As with any modeling study, there are caveats associated with our approach. General caveats related to the downscaling approach or CMIP5 models and experiment design can be found elsewhere in the literature (Emanuel et al., 2006, 2008; Taylor et al., 2012). Furthermore, for this particular study, our choice of models is based on models used in previous work suggesting potential TC track changes near NYC (Garner et al., 2017; Reed, Mann, Emanuel, Lin, et al., 2015). The choice of these models is determined by the availability of necessary thermodynamic and kinematic state variables during the past millennium (Garner et al., 2017), and the limited number of models that meet this criteria may increase the uncertainty associated with our results. During the pre-industrial time period, only the MPI model provides daily wind fields that are necessary for downscaling TC tracks; however, in order to include results from additional models, it is possible to use the monthly values of wind fields included in the IPSL and CCSM4 models. In these cases, variances and covariances of winds are fixed at arbitrarily chosen 1980 CE values, while still allowing winds to vary over the seasonal cycle (Reed, Mann, Emanuel, & Titley, 2015). Such a choice is justified given that simple analyses suggest that long-term variations are well-represented by the fixed co-variance simulation (e.g., see Figure 1 in Reed, Mann, Emanuel, & Titley, 2015). During the modern and future time periods, daily wind fields are provided and used for downscaling TC tracks in all models.

### 4.2. Statistics and Analyses

Density difference maps showing spatial shifts in TC track characteristics (associated with single TC track points) over time are developed using a kernel density estimate in each time period, and then subtracting the two time periods of interest to find the spatial difference over time pertaining to those particular points along TC tracks (Figure 1 and Figures S1, S4, S6 and S7 in Supporting Information S1). Units of the densities shown on these maps are track points per grid cell, where each map has 100 grid cells in both the latitudinal and longitudinal directions. This results in a varying resolution for each map, depending on the latitude and longitude bounds, but no resolution is coarser than 1° longitude by 0.4° latitude.

We use a gridded density calculation to generate maps depicting overall shifts to full TC tracks (Figure S3 in Supporting Information S1 and Figure 5). In this method, a grid is pre-established, and tracks are counted only once in each grid point, ensuring that slow-moving TCs with multiple track points close together are not given undue weight in the regions where they move most slowly, as could happen if using a kernel density estimate to depict full TC tracks rather than individual points from tracks.

Probabilities of TCs associated with Figures 2 and 5 are calculated by determining the total number of TCs in each time period that fall into a particular category (e.g., MDR genesis during the pre-industrial era) and comparing that value to the total number of TCs generated in that time period (e.g., total TCs that form during the pre-industrial era). We do not consider variations in TC frequency in this work, but instead focus on variations in the likelihood of different TC and track characteristics.

Credible intervals (CIs) discussed in the results and shown in Figures 2 and 5 are calculated by generating bootstraps of the original TC data. The bootstrapping technique involves resampling the data sets $n$ times (where $n$ is the number of bootstrap samples) with replacement to produce new samples that are equal in length to the number of samples contained in the original data set (Efron, 1979; Efron & Tibshirani, 1993). For Figure 2, we generate 5,000 bootstrap samples of the TC track characteristics (proximity to NYC, genesis location, termination point, and minimum translation speed) under consideration to determine the 99% CIs ($p = 0.01$). When evaluating the proximity of TCs to various points of interest along the U.S. Atlantic coast, we generate 10,000 bootstrap samples of the probability of TCs traveling within 100 km of each city (NYC, Boston, and Norfolk), which are used to establish both 95% ($p = 0.05$) and 99% CIs ($p = 0.01$).

QQ plots (or Quantile-Quantile plots) are used in several places for analysis, including to assess the time from when a storm forms until it comes within 100 km of a point of interest (Figure 6) and the duration of TC impacts (Figure 7). Such figures plot the quantiles of two distributions against one another (e.g., the distribution of duration of storm impacts at a location during the pre-industrial compared to the distribution of duration of storm impacts at the same location in future). We include a dashed one-to-one line on each figure; points that deviate from this line indicate that the two distributions being compared differ from one another. In Figure 7, the duration of storm impacts at each point of interest is determined by interpolating the 2-hr TC data sets (which include latitude and longitude values, as well as the TC radius of maximum winds) to 15-min time intervals, and then finding the total length of time that the storm's radius of maximum winds exceeds the storm's distance to the point of interest.

To evaluate potential changes to environmental variables associated with changing TC tracks, we use QQ plots to compare distributions of environmental variables for various time periods. In addition, a PCA is used to assess potential relationships between TC track characteristics and environmental conditions.

## Data Availability Statement

Best Track data are available from the Atlantic hurricane database (HURDAT2) at https://www.nhc.noaa.gov/data/hurdat/hurdat2-1851-2020-052921.txt. This work uses simulated TCs downscaled from a model developed by Kerry Emanuel (Massachusetts Institute of Technology), and described in Emanuel et al. (2006, 2008). All inputs to the TC model come from CMIP5 data sets that are publicly available from the Earth System Grid Federation website (https://esgf-node.llnl.gov/projects/cmip5/). Downscaled fields from the TC model, including storm tracks as defined by TC latitude and longitude at 2-hr intervals, are available for research purposes from K. Emanuel (emanuel@mit.edu) on request. Researchers will be asked to sign a non-redistribution agreement and to assert that the data will be used for nonprofit research only.

**Acknowledgments**
The authors wish to thank Kerry Emanuel (Massachusetts Institute of Technology) for the generation and use of synthetic TC data sets for this analysis, and Gregory Garner (Rutgers University) for his code to parse Best Tracks data. This work was supported by funding from the National Science Foundation awarded to A. J. Garner (EAR-1625150) and R. E. Kopp (ICER-1663807). B. P. Horton is supported by the Earth Observatory of Singapore via its funding from the Singapore Ministry of Education Academic Research Fund MOE2019-T3-1-004, the National Research Foundation Singapore, and the Singapore Ministry of Education under the Research Centers of Excellence initiative. This work comprises Earth Observatory of Singapore contribution no. 414.

## References

Alexander, M. A., Scott, J. D., Friedland, K. D., Mills, K. E., Nye, J. A., Pershing, A. J., & Thomas, A. C. (2018). Projected sea surface temperatures over the 21st century: Changes in the mean, variability and extremes for large marine ecosystem regions of Northern Oceans. *Elementa Science of the Anthropocene*, *6*, 9. https://doi.org/10.1525/elementa.191

Avila, L. A., Stewart, S. R., Berg, R., & Hagen, A. B. (2020). *National Hurricane Center tropical cyclone report: Hurricane Dorian*. National Hurricane Center.

Blake, E. S., & Zelinsky, D. A. (2017). *National Hurricane Center tropical cyclone report: Hurricane Harvey*. National Hurricane Center.

Broccoli, A. J., Dahl, K. A., & Stouffer, R. J. (2006). Response of the ITCZ to Northern Hemisphere cooling. *Geophysical Research Letters*, *33*(1). https://doi.org/10.1029/2005GL024546

Burnett, A. C., Sheshadri, A., Silvers, L. G., & Robinson, T. (2021). Tropical cyclone frequency under varying SSTs in aquaplanet simulations. *Geophysical Research Letters*, *48*(5), e2020GL091980. https://doi.org/10.1029/2020GL091980

Camargo, S. J., Emanuel, K. A., & Sobel, A. H. (2007). Use of a genesis potential index to diagnose ENSO effects on tropical cyclone genesis. *Journal of Climate*, *20*(19), 4819–4834. https://doi.org/10.1175/JCLI4282.1

Camargo, S. J., Tippett, M. K., Sobel, A. H., Vecchi, G. A., & Zhao, M. (2014). Testing the performance of tropical cyclone genesis indices in future climates using the HiRAM model. *Journal of Climate*, *27*(24), 9171–9196. https://doi.org/10.1175/JCLI-D-13-00505.1

Chu, J. E., Lee, S. S., Timmermann, A., Wengel, C., Stuecker, M. F., & Yamaguchi, R. (2020). Reduced tropical cyclone densities and ocean effects due to anthropogenic greenhouse warming. *Science Advances*, *6*(51), 5109–5125. https://doi.org/10.1126/sciadv.abd5109

Colbert, A. J., Soden, B. J., Vecchi, G. A., & Kirtman, B. P. (2013). The impact of anthropogenic climate change on North Atlantic tropical cyclone tracks. *Journal of Climate*, *26*(12), 4088–4095. https://doi.org/10.1175/JCLI-D-12-00342.1

Daloz, A. S., Camargo, S. J., Kossin, J. P., Emanuel, K., Horn, M., Jonas, J. A., et al. (2015). Cluster analysis of downscaled and explicitly simulated North Atlantic tropical cyclone tracks. *Journal of Climate*, *28*(4), 1333–1361. https://doi.org/10.1175/JCLI-D-13-00646.1

Efron, B. (1979). Bootstrap methods: Another look at the jackknife. *Annals of Statistics*, *7*, 1–26. https://doi.org/10.1214/aos/1176344552

Efron, B., & Tibshirani, R. J. (1993). *An introduction to the bootstrap*. Chapman and Hall.

Emanuel, K. (1987). The dependence of hurricane intensity on climate. *Nature*, *326*(6112), 483–485. https://doi.org/10.1038/326483a0

Emanuel, K. (2005). Increasing destructiveness of tropical cyclones over the past 30years. *Nature*, *436*(7051), 686–688. https://doi.org/10.1038/nature03906

Emanuel, K. (2011). Global warming effects on U.S. hurricane damage. *Weather, Climate, and Society*, *3*(4), 261–268. https://doi.org/10.1175/WCAS-D-11-00007.1

Emanuel, K., Ravela, S., Vivant, E., & Risi, C. (2006). A statistical deterministic approach to hurricane risk assessment. *Bulletin of the American Meteorological Society*, *87*(3), 299–314. https://doi.org/10.1175/BAMS-87-3-299

Emanuel, K., Sundararajan, R., & Williams, J. (2008). Hurricanes and global warming: Results from downscaling IPCC AR4 simulations. *Bulletin of the American Meteorological Society*, *89*(3), 347–368. https://doi.org/10.1175/BAMS-89-3-347

Garner, A. J., Mann, M. E., Emanuel, K. A., Kopp, R. E., Lin, N., Alley, R. B., et al. (2017). Impact of climate change on New York City's coastal flood hazard: Increasing flood heights from the preindustrial to 2300 CE. *Proceedings of the National Academy of Sciences of the United States of America*, *114*, 11861–11866. https://doi.org/10.1073/pnas.1703568114

Gray, W. M. (1975). *Tropical cyclone genesis*. Colorado State University.

Grinsted, A., Ditlevsen, P., & Christensen, J. H. (2019). Normalized US hurricane damage estimates using area of total destruction, 1900−2018. *Proceedings of the National Academy of Sciences of the United States of America*, *116*, 23942–23946. https://doi.org/10.1073/PNAS.1912277116

Hall, T. M., Kossin, J. P., Thompson, T., & McMahon, J. (2021). U.S. tropical cyclone activity in the 2030s based on projected changes in tropical sea surface temperature. *Journal of Climate*, *34*(4), 1321–1335. https://doi.org/10.1175/JCLI-D-20-0342.1

Halperin, D. J., Hart, R. E., Fuelberg, H. E., & Cossuth, J. H. (2017). The development and evaluation of a statistical-dynamical tropical cyclone genesis guidance tool. *Weather and Forecasting*, *32*(1), 27–46. https://doi.org/10.1175/WAF-D-16-0072.1

Hausfather, Z., & Peters, G. P. (2020). Emissions—The "business as usual" story is misleading. *Nature*, *577*(7792), 618–620. https://doi.org/10.1038/d41586-020-00177-3

Kemp, A. C., & Horton, B. P. (2013). Contribution of relative sea-level rise to historical hurricane flooding in New York City. *Journal of Quaternary Science*, *28*(6), 537–541. https://doi.org/10.1002/jqs.2653

Knutson, T. R., Camargo, S. J., Chan, J. C. L., Emanuel, K., Ho, C.-H., Kossin, J., et al. (2019). Tropical cyclones and climate change assessment: Part II. Projected response to anthropogenic warming. *Bulletin of the American Meteorological Society*, *101*(3), 303–322. https://doi.org/10.1175/BAMS-D-18-0194.1

Knutson, T. R., Sirutis, J. J., Zhao, M., Tuleya, R. E., Bender, M., Vecchi, G. A., et al. (2015). Global projections of intense tropical cyclone activity for the late twenty-first century from dynamical downscaling of CMIP5/RCP4.5 scenarios. *Journal of Climate*, *28*(18), 7203–7224. https://doi.org/10.1175/JCLI-D-15-0129.1

Kossin, J. P. (2017). Hurricane intensification along United States coast suppressed during active hurricane periods. *Nature*, *541*(7637), 390–393. https://doi.org/10.1038/nature20783

Kossin, J. P. (2018). A global slowdown of tropical-cyclone translation speed. *Nature*, *558*(7708), 104–107. https://doi.org/10.1038/s41586-018-0158-3

Kossin, J. P., Camargo, S. J., & Sitkowski, M. (2010). Climate modulation of north Atlantic hurricane tracks. *Journal of Climate*, *23*(11), 3057–3076. https://doi.org/10.1175/2010JCLI3497.1

Kossin, J. P., Emanuel, K. A., & Camargo, S. J. (2016). Past and projected changes in western north pacific tropical cyclone exposure. *Journal of Climate*, *29*(16), 5725–5739. https://doi.org/10.1175/JCLI-D-16-0076.1

Kossin, J. P., Emanuel, K. A., & Vecchi, G. A. (2014). The poleward migration of the location of tropical cyclone maximum intensity. *Nature*, *509*(7500), 349–352. https://doi.org/10.1038/nature13278

Kozar, M. E., Mann, M. E., Emanuel, K. A., & Evans, J. L. (2013). Long-term variations of North Atlantic tropical cyclone activity downscaled from a coupled model simulation of the last millennium. *Journal of Geophysical Research: Atmospheres*, *118*(24), 13383–13392. https://doi.org/10.1002/2013JD020380

Lai, Y., Li, J., Gu, X., Chen, Y. D., Kong, D., Gan, T. Y., et al. (2020). Greater flood risks in response to slowdown of tropical cyclones over the coast of China. *Proceedings of the National Academy of Sciences of the United States of America*, *117*(26), 14751–14755. https://doi.org/10.1073/pnas.1918987117

Landsea, C. W., & Franklin, J. L. (2013). Atlantic hurricane database uncertainty and presentation of a new database format. *Monthly Weather Review*, *141*(10), 3576–3592. https://doi.org/10.1175/MWR-D-12-00254.1

Lin, N., Emanuel, K., Oppenheimer, M., & Vanmarcke, E. (2012). Physically based assessment of hurricane surge threat under climate change. *Nature Climate Change*, *2*(6), 462–467. https://doi.org/10.1038/nclimate1389

Lin, N., Kopp, R. E., Horton, B. P., & Donnelly, J. P. (2016). Hurricane Sandy's flood frequency increasing from year 1800 to 2100. *Proceedings of the National Academy of Sciences of the United States of America*, *113*(43), 12071–12075. https://doi.org/10.1073/pnas.1604386113

Lin, N., Smith, J. A., Villarini, G., Marchok, T. P., & Baeck, M. L. (2010). Modeling extreme rainfall, winds, and surge from hurricane Isabel (2003). *Weather and Forecasting*, *25*(5), 1342–1361. https://doi.org/10.1175/2010WAF2222349.1

Lucas, C., Timbal, B., & Nguyen, H. (2014). The expanding tropics: A critical assessment of the observational and modeling studies. In: *Wiley interdisciplinary reviews: Climate change*. Wiley-Blackwell. https://doi.org/10.1002/wcc.251

Marsooli, R., Lin, N., Emanuel, K., & Feng, K. (2019). Climate change exacerbates hurricane flood hazards along US Atlantic and Gulf Coasts in spatially varying patterns. *Nature Communications*, *10*(1), 1–9. https://doi.org/10.1038/s41467-019-11755-z

Mendelsohn, R., Emanuel, K., Chonabayashi, S., & Bakkensen, L. (2012). The impact of climate change on global tropical cyclone damage. *Nature Climate Change*, *2*(3), 205–209. https://doi.org/10.1038/nclimate1357

Murakami, H., Mizuta, R., & Shindo, E. (2012). Future changes in tropical cyclone activity projected by multi-physics and multi-SST ensemble experiments using the 60-km-mesh MRI-AGCM. *Climate Dynamics*, *39*, 2569–2584. https://doi.org/10.1007/s00382-011-1223-x

Nakamura, J., Camargo, S. J., Sobel, A. H., Henderson, N., Emanuel, K. A., Kumar, A., et al. (2017). Western North Pacific tropical cyclone model tracks in present and future climates. *Journal of Geophysical Research: Atmospheres*, *122*(18), 9721–9744. https://doi.org/10.1002/2017JD027007

National Research Council. (2013). Committee on assessing the impact of climate change on social and political stresses. In *Climate and social stress: Implications for security analysis*. The National Academies.

NOAA National Centers for Environmental Information. (NCEI). (2020). *U.S. Billion-dollar weather and climate disasters*. Retrieved from https://www.ncdc.noaa.gov/billions/

Pielke, R. A. (2007). Future economic damage from tropical cyclones: Sensitivities to societal and climate changes. *Philosophical Transactions of the Royal Society A: Mathematical, Physical & Engineering Sciences*, *365*(1860), 2717–2729. https://doi.org/10.1098/rsta.2007.2086

Rappaport, E. N. (2014). Fatalities in the United States from Atlantic tropical cyclones: New data and interpretation. *Bulletin of the American Meteorological Society*, *95*(3), 341–346. https://doi.org/10.1175/BAMS-D-12-00074.1

Reed, A. J., Mann, M. E., Emanuel, K. A., Lin, N., Horton, B. P., Kemp, A. C., & Donnelly, J. P. (2015). Increased threat of tropical cyclones and coastal flooding to New York City during the anthropogenic era. *Proceedings of the National Academy of Sciences of the United States of America*, *112*(41), 12610–12615. https://doi.org/10.1073/pnas.1513127112

Reed, A. J., Mann, M. E., Emanuel, K. A., & Titley, D. W. (2015). An analysis of long-term relationships among count statistics and metrics of synthetic tropical cyclones downscaled from CMIP5 models. *Journal of Geophysical Research: Atmospheres*, *120*(15), 7506–7519. https://doi.org/10.1002/2015JD023357

Riahi, K., Rao, S., Krey, V., Cho, C., Chirkov, V., Fischer, G., et al. (2011). RCP 8.5—A scenario of comparatively high greenhouse gas emissions. *Climatic Change*, *109*(1–2), 33–57. https://doi.org/10.1007/s10584-011-0149-y

Seneviratne, S. I., Zhang, X., Adnan, M., Badi, W., Dereczynski, C., Di Luca, A., et al. (2021). Weather and climate extreme events in a changing climate. In: In V. Masson-Delmotte, P. Zhai, A. Pirani, S. Connors, C. Pean, S. Berger, et al. (Eds.), *Climate change 2021: The physical science basis. Contribution of working group I to the sixth assessment report of the intergovernmental panel on climate change*. Cambridge University Press.

Stocker, T. F., Qin, D., Plattner, G.-K., Alexander, L. V., Allen, S. K., Bindoff, N. L., et al. (2013). Technical summary—IPCC. In: In T. F. Stocker, D. Qin, G.-K. Plattner, M. Tignor, S. K. Allen, J. Boschung, et al. (Eds.), *Climate change 2013: The physical science basis. Contribution of working group I to the fifth assessment report of the intergovernmental panel on climate change*. Cambridge University Press. Retrieved from https://www.ipcc.ch/report/ar5/wg1/technical-summary/

Taylor, K. E., Stouffer, R. J., & Meehl, G. A. (2012). An overview of CMIP5 and the experiment design. *Bulletin of the American Meteorological Society*, *93*(4), 485–498. https://doi.org/10.1175/BAMS-D-11-00094.1

Ting, M., Kossin, J. P., Camargo, S. J., & Li, C. (2019). Past and future hurricane intensity change along the U.S. East Coast. *Scientific Reports*, *9*(1), 7795. https://doi.org/10.1038/s41598-019-44252-w

U.S. Navy. (2020). *Naval Station Norfolk*. Retrieved from https://www.cnic.navy.mil/regions/cnrma/installations/ns_norfolk.html

Van Hengstum, P. J., Donnelly, J. P., Fall, P. L., Toomey, M. R., Albury, N. A., & Kakuk, B. (2016). The Intertropical Convergence Zone modulates intense hurricane strikes on the western North Atlantic margin. *Scientific Reports*, *6*, 21728. https://doi.org/10.1038/srep21728

Villarini, G., & Vecchi, G. A. (2013). Projected increases in North Atlantic tropical cyclone intensity from CMIP5 models. *Journal of Climate*, *26*(10), 3231–3240. https://doi.org/10.1175/JCLI-D-12-00441.1

Wahl, T., Jain, S., Bender, J., Meyers, S. D., & Luther, M. E. (2015). Increasing risk of compound flooding from storm surge and rainfall for major US cities. *Nature Climate Change*, *5*(12), 1093–1097. https://doi.org/10.1038/nclimate2736

Wang, S., & Toumi, R. (2021). Recent migration of tropical cyclones toward coasts. *Science*, *371*(6528), 514–517. https://doi.org/10.1126/science.abb9038

Zhang, G., Murakami, H., Knutson, T. R., Mizuta, R., & Yoshida, K. (2020). Tropical cyclone motion in a changing climate. *Science Advances*, *6*(17), 7610–7632. https://doi.org/10.1126/sciadv.aaz7610